

1 Distal turbidites reveal a common distribution for large
2 ($>0.1 \text{ km}^3$) submarine landslide recurrence

3 **Michael A. Clare¹, Peter J. Talling¹, Peter Challenor², Giuseppe Malgesini¹, and**
4 **James Hunt¹**

5 ¹*National Oceanography Centre, Southampton, European Way, Southampton SO14 3ZH,*
6 *UK*

7 ²*College of Engineering, Mathematics and Physical Sciences, University of Exeter, North*
8 *Park Road, Exeter EX4 4QF, UK*

9 **ABSTRACT**

10 Submarine landslides can be far larger than those on land, and are one of the most
11 important processes for moving sediment across our planet. Landslides that are fast
12 enough to disintegrate can generate potentially very hazardous tsunamis, and produce
13 long run-out turbidity currents that break strategically important cable networks. It is
14 important to understand their frequency and triggers. We document the distribution of
15 recurrence intervals for large landslide-triggered turbidity currents ($>0.1 \text{ km}^3$) in three
16 basin-plains. A common distribution of recurrence intervals is observed, despite variable
17 ages and disparate locations, suggesting similar underlying controls on slide triggers and
18 frequency. This common distribution closely approximates a temporally-random Poisson
19 distribution, such that the probability of a large disintegrating slide occurring along the
20 basin margin is independent of the time since the last slide. This distribution suggests that
21 non-random processes such as sea level are not a dominant control on frequency of these
22 slides. Recurrence intervals of major ($>M 7.3$) earthquakes have an approximately

23 Poissonian distribution, suggesting they could be implicated as triggers. However, not all
24 major earthquakes appear to generate widespread turbidites, and other as yet unknown
25 triggers or sequential combinations of processes could produce the same distribution.
26 This is the first study to show that large slide-triggered turbidites have a common
27 frequency distribution in distal basin plains, and that this distribution is temporally
28 random. This result has important implications for assessing hazards from landslide-
29 tsunamis and seafloor cable breaks, and the long-term tempo of global sediment fluxes.

30 **INTRODUCTION**

31 Submarine landslides (hereafter “slides”) on continental margins include the
32 largest mass flows on Earth. They can involve hundreds to several thousand cubic
33 kilometers of material (Hühnerbach and Masson, 2004), and be far larger than those on
34 land. Many large slides initiate on sea floor gradients of $<2^\circ$ that would almost always be
35 stable on land (Urlaub et al., 2013). Motion of the slide can potentially generate
36 damaging tsunamis that travel across the ocean for long distances. Mixing of the slide
37 mass with the surrounding seawater can form longer run-out sediment flows called
38 turbidity currents, which can travel for hundreds of kilometers, sometimes with speeds of
39 up to 19 m/s (Piper et al., 1999). Cables that carry over 95% of transoceanic global data
40 (Carter et al., 2009), and expensive oil and gas infrastructure may be damaged by slides
41 and turbidity currents. The most hazardous events are large volume and fast moving
42 slides that disintegrate to produce turbidity currents. They are also the most important
43 events for transporting sediment over long distances. We consider deposit volumes >0.1
44 km^3 as representing large slides—although some slides can be up to three orders of
45 magnitude larger (Urlaub et al., 2013). Determining whether large-volume slides have a

46 common frequency distribution, and what that distribution may be, has importance for
47 understanding global sediment fluxes and regional hazards associated with tsunamis and
48 damage to seafloor structures. The frequency distribution can also provide insights into
49 triggers and preconditioning factors.

50 Numerous hypotheses have been proposed for how large submarine slides are
51 triggered and slopes are preconditioned to fail. However, we are yet to monitor a large
52 slide in action, and these hypotheses remain poorly tested. Rapid accumulation of
53 impermeable sediment is often invoked as a preconditioning factor for failure, which may
54 then be triggered by an earthquake (Stigall and Dugan, 2010). However, very large slides
55 also occur in areas of slow sedimentation (Urlaub et al., 2013), failure may occur
56 thousands of years after rapid sedimentation ceases (Leynaud et al., 2009), and some
57 recent large earthquakes did not produce widespread slope failure (Sumner et al., 2013;
58 Völker et al., 2011). The headwalls of most large slides are too deep (> 200 m water
59 depth) for triggering by cyclic wave loading, and some headwalls are too deep (>2000 m)
60 for triggering by gas hydrate dissociation (Hühnerbach and Masson, 2004). It has been
61 suggested that sea-level changes play a key role in preconditioning or triggering slope
62 failure (Lee, 2009). However, a recent analysis of large slide frequency concluded that
63 there was no significant association with sea level (Urlaub et al., 2013).

64 **Aims**

65 We aim to determine the frequency distribution of recurrence intervals for
66 turbidites triggered by large (>0.1 km³) submarine slides in three deep-sea basins. As a
67 similar frequency distribution of recurrence intervals is observed, we explore the
68 significance of this distribution for understanding how large slides are triggered. This

69 analysis includes potential triggering of slides by sea level changes and large magnitude
70 earthquakes.

71 **METHODS**

72 It can be difficult to document slide ages precisely by dating sediment
73 immediately above and below the slide deposit, even when samples are recent enough to
74 be radiocarbon dated (Urlaub et al., 2013). Dated samples are also needed from different
75 lobes of a slide deposit to check whether they were emplaced by a single slide, or
76 multiple slides with variable ages. We therefore use an alternative method for
77 documenting time periods between large slides around a basin margin, using turbidity
78 current deposits ('turbidites') generated by the slides. The recurrence time of slides is
79 inferred from intervals of hemipelagic mud that settles out between turbidity currents,
80 and average accumulation rate of the hemipelagic mud. This provides information on
81 timing of many (>100) slides, which aids robust statistical analysis. It avoids the need to
82 date prohibitively large numbers of slides, each in a different location on the margin.

83 **Study Areas**

84 Turbidite sequences in three deep-water basin plains are considered (Fig. 1; see
85 the GSA Data Repository¹), including the Madeira Abyssal Plain (offshore northwest
86 Africa), the Balearic Abyssal Plain (western Mediterranean Sea), and the Marnoso-
87 arenacea Formation (Italian Apennines). The Madeira Abyssal Plain record comes from
88 Ocean Drilling Program (ODP) cores and spans the past ~7 m.y., while piston coring of
89 the Balearic Abyssal Plain provides a sequence for the past ~150 k.y. Outcrops of the
90 Marnoso-arenacea Formation provide a record of events between 13.5 and 14.1 Ma.
91 There are few (if any) other locations worldwide that fulfill the following key criteria

92 needed for this approach; that there are a sufficient number ($> \sim 100$) of turbidites for
93 robust statistical analyses, hemipelagic mud can be easily distinguished from turbidite
94 mud in the field, and there is evidence that erosion was limited below turbidites.

95 **Age Control**

96 It was not feasible to date every hemipelagic mud interval. The time period
97 between turbidites was derived by dividing the thickness of hemipelagic mud between
98 turbidites by the average hemipelagic mud accumulation rate. This accumulation rate was
99 calculated between adjacent dated horizons by dividing their difference in age by
100 cumulative hemipelagic mud thickness. Detail on the dating methods for each data set is
101 provided in the Data Repository, together with analysis of effects of short-term variations
102 in hemipelagic accumulation rate.

103 **Distinguishing Hemipelagic Mud and Turbidite Mud**

104 It is essential to be able to distinguish between mud deposited by hemipelagic
105 fallout and turbidity currents, in order to measure the thickness of hemipelagic mud
106 between each turbidite and hence calculate recurrence times. The three data sets were
107 chosen because the two types of mud have distinctive features and colors (Fig. DR1 in
108 the Data Repository). It is often very difficult to identify the two types of mud (Talling et
109 al., 2012). Visually diagnostic features of hemipelagic mud in our sequences are common
110 dispersed foraminifera, reduced organic carbon content, higher calcium carbonate
111 content, lighter color and bioturbation (Table DR1). This visual differentiation is
112 consistent with detailed geochemical (Rothwell et al., 2004), and microscopic analyses
113 (Talling et al., 2007).

114 **Erosion by Turbidity Currents**

115 Our method requires that significant thicknesses of hemipelagic mud were not
116 eroded beneath turbidity currents, and we show how erosion would affect recurrence time
117 estimates in the Data Repository. This view is supported by mapping of hemipelagic mud
118 thickness beneath individual beds in the Marnoso-arenacea Formation, showing that this
119 thickness varies by <5–10 cm over ~120 km (Fig. DR1). A lack of spatial variation in
120 coccolith assemblages and thickness of turbidite mud caps in the Madeira Abyssal Plain
121 indicate minimal erosion—interpreted to be less than a few centimeters (Weaver and
122 Thomson, 1993). The turbidite beds in the Madeira and Balearic Abyssal Plain cores lack
123 irregular bases indicative of erosion, although the narrow core width (<10 cm) precludes
124 observation of larger-scale erosional features.

125 **Short-term Fluctuations in Hemipelagic Mud Accumulation Rates**

126 Our method for calculating recurrence intervals assumes that no significant
127 fluctuation in hemipelagic mud accumulation rates occurred between dated horizons.
128 Such horizons occur every 0.4 k.y. to 18.5 k.y. in the Balearic Abyssal Plain, and every 5
129 k.y. to 1 m.y. in the Madeira Abyssal Plain. This issue is most important for the Marnoso-
130 arenacea Formation, where a constant hemipelagic accumulation rate is assumed over the
131 entire interval. This assumption may not be unreasonable, as hemipelagic accumulation
132 rates in the Balearic Plain only vary by ~30% over an interval of 150 k.y.

133 **Were These Extensive Basin Plain Turbidity Currents Triggered by Large** 134 **Landslides?**

135 It is known that slope failures can generate turbidity currents that reach distal
136 basin plains, from often very large slides on the open continental slope (Piper et al., 1999)
137 or smaller failures that lead to canyon flushing flows (Piper and Savoye, 1993; Talling et

138 al., 2012). However, it is possible that flows reaching basin plains can be triggered in
139 other ways. Turbidite volume provides the best evidence of triggering by slope failure, as
140 other triggers most likely produce small ($<0.1 \text{ km}^3$) sediment volume flows. Even the
141 largest flood discharges into the ocean tend to involve $<0.1 \text{ km}^3$ of sediment (Dadson et
142 al., 2005), although such flood-triggered submarine flows could pick up sediment en-
143 route to basin plains. The data sets considered here were chosen because each turbidite
144 contains large ($>0.1 \text{ km}^3$ to 500 km^3) volumes of sediment (Tables DR3–DR5). Volume
145 estimates are based on unusually detailed long distance ($>100 \text{ km}$) mapping of individual
146 beds in the Marnoso-arenacea Formation, the Madeira Abyssal Plain and the Balearic
147 Abyssal Plain (Table DR1). However, even if these turbidity currents were generated by
148 floods and eroded very large sediment volumes during canyon flushing, understanding
149 their recurrence times is still important for geohazards to seafloor infrastructure.

150 Not all slides trigger long run-out turbidity currents, as some slides may be too
151 slow moving to disintegrate. This study only considers faster-moving and larger slides
152 that disintegrate to produce voluminous turbidites. It is these events that pose the greatest
153 regional threat to seafloor infrastructure, may produce hazardous tsunamis, and are most
154 important for continental margin evolution and global sediment transport.

155

156 **RESULTS**

157 **Common Frequency Distribution of Landslide-Turbidite Recurrence Intervals**

158 The recurrence interval distributions form a nearly straight line on a log-linear
159 exceedence plot for all three data sets (Fig. 1). This linear trend indicates an exponential
160 relationship, characteristic of a Poisson distribution, although there is a slight deviation

161 for the longest recurrence intervals. A Poisson distribution implies a lack of memory,
162 such that the probability of a new event occurring is independent of the time since the
163 last. It is characterized by only one parameter (λ)—the mean recurrence interval or rate
164 parameter. Equation 1 defines the Probability Function (P) that a discrete random
165 recurrence interval (X) is less than a specific value for the data series (x). The solution is
166 related to an exponential function (e^x) and the rate parameter (λ). Values of X , x , and λ
167 are integers defined in thousands of years.

$$168 \quad P(X < x) = 1 - e^{-\frac{x}{\lambda}}. \quad (1)$$

169 A common distribution in data sets from multiple disparate settings may indicate
170 a common underlying control, and this has not been shown previously for large slide-
171 triggered turbidites preserved in distal basin plains.

172 **Is This Distribution Temporally Random (Poissonian)?**

173 To test that the data are truly exponential and they share a common distribution,
174 they are normalized by sub-dividing each recurrence interval, T , by mean recurrence
175 interval (λ) for each of the data sets to plot a dimensionless variable, R_T . The data sets
176 show close agreement when plotted in this way, despite disparity in their age, location
177 and setting. R_T values closely approximate an exponential distribution; however, some
178 slight overpopulation is observed at the tail for $R_T > 3$, suggesting a small deviation from
179 a strictly Poisson distribution.

180 To test whether this is a Poisson distribution, a Generalized Linear Model is
181 applied to the data using a Gamma distribution (of which the exponential is a special
182 function). This defines a dispersion parameter, α , for the curve fitted to each of the data
183 sets. A true exponential distribution is represented by $\alpha = 1$; however, values between 1

184 and 2 can be treated as Poissonian. The values derived for the data sets in this study are
185 between 1.03 and 1.21. This indicates that they are near-exponentially distributed, albeit
186 with some overpopulation in the tail of the data.

187 **Effects of Variable Erosion Beneath Beds**

188 We now explore how erosion of hemipelagic mud to variable depths by turbidity
189 currents could potentially influence our results. Random amounts of erosion to depths of
190 0–10 cm are simulated for the original hemipelagic mud thickness data (Fig. DR1). This
191 depth range was chosen as it is the maximum difference in hemipelagic mud thickness
192 beneath Marnoso-arenacea turbidites mapped over 120 km (Talling et al., 2007).
193 Additional erosion was only simulated below turbidites that are equal or thicker than the
194 mean turbidite thickness, rather than beneath every turbidite. Erosion is likely to be
195 greater beneath thicker beds, which represent larger and more powerful turbidity currents.
196 Accounting for differential erosion also provides a near-exponential distribution. This
197 supports the view that erosion of up to 10 cm between beds would not modify our main
198 conclusion that recurrence times approximate a Poisson distribution.

199 **Effects of Short-Term Changes in Hemipelagic Accumulation Rates**

200 Random variations between $\pm 50\%$ of the mean recurrence interval between
201 turbidites were applied to the data from the Madeira Abyssal Plain (Fig. DR1). This
202 simulates short-term temporal variations in hemipelagic accumulation rates. A near-
203 exponential distribution of inter-event times is still observed.

204 **DISCUSSION**

205 We first discuss the implications of the observed Poisson distribution for
206 understanding triggers and preconditioning factors for large disintegrative slides.

207 **Geological Significance of Poisson Distribution**

208 A Poisson distribution results from a process that is random and lacks memory, in
209 the sense that the probability of an event occurring is independent of the time since the
210 last. A Poisson distribution of landslide-turbidite frequency could form in three ways.
211 First, the distribution could result from a single basin-wide triggering process that is
212 randomly distributed in time. Second, it could result from numerous different basin-wide
213 triggers, or from many different triggering processes that each affects a localized area
214 along the basin margin. Third, it could result from a sequential chain of multiple
215 processes, each occurring one after the other. The Poisson distribution suggests that
216 triggering of landslide-turbidites is not due to a single process, or a small number of
217 processes, whose distribution is non-random through time.

218 **Landslide-Turbidite Frequency and Sea Level**

219 It has been proposed that glacial-eustatic sea-level fluctuations are a major control
220 on the frequency of large slides (Lee, 2009). However, all three data sets show no
221 evidence for a strong eustatic sea level control that is not temporally random. This
222 suggests that sea level is not a major triggering or preconditioning factors for large
223 disintegrative slides. Such a view is consistent with a recent global analysis of large slide
224 ages during the past 30 k.y. (Urlaub et al., 2013), but is contrary to that of previous
225 workers (e.g., Lee, 2009). Processes that fluctuate in conjunction with eustatic sea level
226 and climate cycles are also unlikely to be temporally random, and this study suggests that
227 they too are not dominant single controls on slide timing. Such process may include
228 dissociation of gas hydrates due to ocean warming, or increased sedimentation rates on
229 continental slopes during sea-level lowstands.

230 **Comparison to the Frequency Distribution of Large Magnitude Earthquakes**

231 It has been proposed that recurrence intervals of large magnitude ($M > 7.3$)
232 earthquakes in global databases, documented by seismometers since ca. A.D. 1900, are
233 temporally random and follow a Poisson distribution (Corral, 2006). These analyses
234 exclude aftershocks. Other workers have argued that this instrumental record contains too
235 few events to be sure that the distribution is Poissonian (e.g., Daub et al., 2012). This
236 result is only found for measurements made over large areas, as individual fault segments
237 can have characteristic earthquake recurrence periods.

238 It might therefore be suggested that large slides are triggered by major
239 earthquakes, based on the similarity between the shape of the frequency distribution of
240 recurrence intervals of slide-turbidites and large magnitude earthquakes (Fig. DR2). In
241 contrast, the frequency distribution of river floods is far from an exponential Poisson
242 distribution (Bobée et al., 1993). Although some large slides are known to have been
243 triggered by earthquakes (Piper et al., 1999), some large (M 8.4 and 9.1) earthquakes do
244 not always cause widespread seafloor failure (Sumner et al., 2013; Völker et al., 2011).
245 This suggests that only a subset of major earthquakes trigger large slides, such that there
246 is not a one-to-one correlation between major earthquakes and large slides. This view is
247 consistent with the average recurrence intervals recorded here (1.4–36.5 k.y.), which tend
248 to be significantly longer than average historical recurrence intervals of major ($>M$ 7.3)
249 earthquakes of tens to several hundred years (e.g., Meghraoui et al., 1988). It could then
250 be argued that only very large magnitude (M 8 or 9) earthquakes trigger slides, but field
251 observations suggest that sometimes even these do not produce extensive slides (Sumner
252 et al., 2013; Völker et al., 2011).

253 **Multiple Local or Sequential Controls Along Basin Margin**

254 It is also possible that slides are mainly triggered by one or more currently
255 unknown factors that have a Poisson distribution, or that different factors trigger slides
256 locally along the margin. The latter view implies that there is not a single dominant
257 source location for most turbidites in a basin-floor data set, and slides are triggered in
258 variable ways at different points around the margin. This results in a temporally-random,
259 regionalized sum of slide recurrence times. However, a rigorous test of this model is
260 problematic as the source of each turbidite in our data sets cannot be pinpointed with
261 sufficient precision. It is also possible that a temporally random distribution may result
262 from cumulative triggering by a series of factors that occur one after another, at a single
263 location.

264 **CONCLUSIONS**

265 Analysis of large volume turbidites ($>0.1 \text{ km}^3$) in three basin plains indicates that
266 there is a common frequency distribution of inter-event times for larger and faster-
267 moving slides that disintegrate. Such slides tend to form relatively large tsunamis, pose
268 the greatest regional hazard to seafloor infrastructure, and are most important for global
269 sediment fluxes. This novel conclusion may indicate similar controls on slide frequency
270 and triggers occur in disparate areas. The common frequency distribution approximates a
271 Poisson distribution, such that the time to the next slide is independent of the time since
272 the last. This suggests that temporally non-random processes, such as glacio-eustatic sea-
273 level change, are not dominant single controls on slide frequency, contrary to the
274 conclusions of some previous work. It appears that processes that fluctuate in conjunction
275 with eustatic sea-level and climate cycles (e.g., shelf edge sedimentation rates or hydrate

276 dissociation driven by ocean warming) are also not dominant single controls on slide
277 timing. Major earthquakes have an approximately Poisson distribution of recurrence
278 intervals suggesting they may play a role in slide triggering, although not all major
279 earthquakes appear to generate large disintegrating slides. Alternatively, slides may be
280 triggered by processes that are yet unknown which are temporally random, by many
281 disparate processes acting locally along a basin margin, or by a series of processes that
282 occur one after another at a single location. It is feasible that our records may also include
283 large volume canyon flushing events; however, regardless of this, our study has important
284 implications for predicting frequency of landslide-tsunamis, the occurrence of cable
285 breaks, and the global tempo of sediment transport. It suggests that the frequency of large
286 volume flows, such as those triggered by disintegrative landslides is unlikely to change
287 significantly due to rapid eustatic sea-level rise during forthcoming decades.

288 **ACKNOWLEDGMENTS**

289 We thank three anonymous reviewers for suggestions that greatly improved
290 the manuscript, and Alessandra Negri who performed biostratigraphic analyses at the
291 Marnoso-arenacea section.

292 **REFERENCES CITED**

- 293 Bobée, B., Cavadia, G., Ashkar, F., Bernier, J., and Rasmussen, P., 1993, Towards a
294 systematic approach to comparing distributions used in flood frequency analysis:
295 Journal of Hydrology (Amsterdam), v. 142, p. 121–136, doi:10.1016/0022-
296 1694(93)90008-W.
- 297 Carter, L., Burnett, D., Drew, S., Marle, G., Hagadorn, L., Bartlett-McNeil, D., and
298 Irvine, N., 2009, Submarine Cables and the Oceans—Connecting the World: United

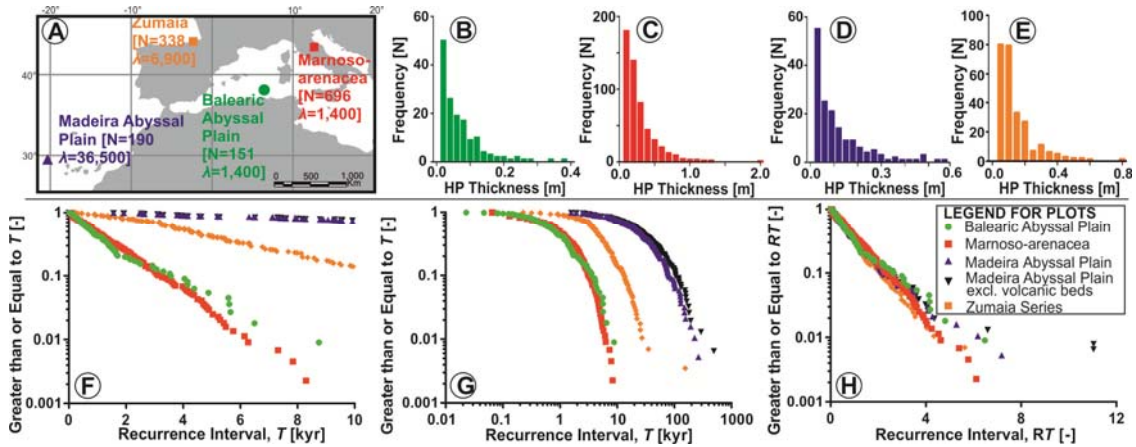
- 299 Nations Environment Programme, World Conservation Monitoring Center (UNEP-
300 WCMC) Biodiversity Series No. 31: Cambridge, UK, United Nations Environment
301 Programme, World Conservation Monitoring Center: [http://www.unep-](http://www.unep-wcmc.org/resources/publications/UNEP_WCMC_bio_series/31.aspx)
302 [wcmc.org/resources/publications/UNEP_WCMC_bio_series/31.aspx](http://www.unep-wcmc.org/resources/publications/UNEP_WCMC_bio_series/31.aspx) (accessed
303 November 2013).
- 304 Corral, A., 2006, Dependence of earthquake recurrence times and independence of
305 magnitudes on seismicity history: *Tectonophysics*, v. 424, p. 177–193,
306 doi:10.1016/j.tecto.2006.03.035.
- 307 Dadson, S.J., Hovius, N., Pegg, S., Dade, W.B., and Horng, M.J., 2005, Hyperpycnal
308 river flows from an active mountain belt: *Journal of Geophysical Research*, v. 110,
309 p. F04016, doi:10.1029/2004JF000244.
- 310 Daub, E.G., Ben-Naim, E., Guyer, R.A., and Johnson, P.A., 2012, Are megaquakes
311 clustered?: *Geophysical Research Letters*, v. 39, doi:10.1029/2012GL051465.
- 312 Hühnerbach, V., and Masson, D.G., 2004, Landslides in the North Atlantic and its
313 adjacent seas: An analysis of their morphology, setting and behaviour: *Marine*
314 *Geology*, v. 213, p. 343–362, doi:10.1016/j.margeo.2004.10.013.
- 315 Lee, H.J., 2009, Timing of occurrence of large submarine landslides on the Atlantic
316 Ocean margin: *Marine Geology*, v. 264, p. 53–64,
317 doi:10.1016/j.margeo.2008.09.009.
- 318 Leynaud, D., Mienert, J., and Vanneste, M., 2009, Submarine mass movements on
319 glaciated and non-glaciated European continental margins: A review of triggering
320 mechanisms and preconditions to failure: *Marine and Petroleum Geology*, v. 26,
321 p. 618–632, doi:10.1016/j.marpetgeo.2008.02.008.

- 322 Meghraoui, M., Jaegy, R., Lammali, K., and Alberede, F., 1988, Late Holocene
323 earthquake sequences on the El Asnam (Algeria) thrust fault: *Earth and Planetary*
324 *Science Letters*, v. 90, p. 187–203, doi:10.1016/0012-821X(88)90100-8.
- 325 Piper, D.J.W., and Savoye, B., 1993, Processes of Late Quaternary turbidity-current flow
326 and deposition on the Var deep-sea fan, North-west Mediterranean Sea:
327 *Sedimentology*, v. 40, p. 557–582, doi:10.1111/j.1365-3091.1993.tb01350.x.
- 328 Piper, D.J.W., Cochonat, P., and Morrison, M.L., 1999, The sequence of events around
329 the epicenter of the 1929 Grand Banks earthquake: Initiation of the debris flows and
330 turbidity current inferred from side scan sonar: *Sedimentology*, v. 46, p. 79–97,
331 doi:10.1046/j.1365-3091.1999.00204.x.
- 332 Rothwell, R.G., Hoogakker, B., Thomson, J., Croudace, I.W., and Frenz, M., 2004,
333 Turbidite emplacement on the southern Balearic Abyssal Plain (western
334 Mediterranean Sea) during Marine Isotope Stages 1–3: An application of ITRAX
335 XRF scanning of sediment cores to lithostratigraphic analysis, *in* Rothwell, R.G., ed.,
336 *New Techniques in Sediment Core Analysis: Geological Society of London Special*
337 *Publication 267*, p. 79–98.
- 338 Stigall, J., and Dugan, B., 2010, Overpressure and earthquake initiated slope failure in the
339 Ursa region, northern Gulf of Mexico: *Journal of Geophysical Research*, v. 115,
340 p. B04101, doi:10.1029/2009JB006848.
- 341 Sumner, E.J., Siti, M.I., McNeill, L.C., Talling, P.J., Henstock, T.J., Wynn, R.B.,
342 Djajadihardja, Y.S., and Permana, H., 2013, Can turbidites be used to reconstruct a
343 palaeoearthquake record for the central Sumatran margin?: *Geology*, v. 41, p. 763–
344 766, doi:10.1130/G34298.1.

- 345 Talling, P.J., Amy, L.A., Wynn, R.B., Blackbourn, G., and Gibson, O., 2007, Evolution
346 of turbidity currents deduced from extensive thin turbidites: Marnoso Arenacea
347 formation (Miocene), Italian Apennines: *Journal of Sedimentary Research*, v. 77,
348 p. 172–196, doi:10.2110/jsr.2007.018.
- 349 Talling, P.J., Masson, D.G., Sumner, E.J., and Malgesini, G., 2012, Subaqueous sediment
350 density flows: Depositional processes and deposit types: *Sedimentology*, v. 59,
351 p. 1937–2003, doi:10.1111/j.1365-3091.2012.01353.x.
- 352 Urlaub, M., Talling, P.J., and Masson, D.G., 2013, Timing and frequency of large
353 submarine landslides: Implications for understanding triggers and future geohazard:
354 *Quaternary Science Reviews*, v. 72, p. 63–82, doi:10.1016/j.quascirev.2013.04.020.
- 355 Völker, D., Scholz, F., and Geerson, J., 2011, Analysis of submarine landsliding in the
356 rupture area of the 27 February 2010 Maule earthquake, Central Chile: *Marine*
357 *Geology*, v. 288, p. 79–89, doi:10.1016/j.margeo.2011.08.003.
- 358 Weaver, P.P.E., and Thomson, J., 1993, Calculating erosion by deep-sea turbidity
359 currents during initiation and flow: *Nature*, v. 364, p. 136–138,
360 doi:10.1038/364136a0.
- 361

362 **FIGURE CAPTION**

363 Figure 1. A: Location map. B–D: Frequency histograms of hemipelagic mud thickness.
364 E–G: Recurrence intervals plotted on log-linear axes (E), log-log axes (F), and with
365 recurrence intervals normalized by rate parameter (λ) (G).



366

367

368 ¹GSA Data Repository item 2014xxx, available chronostratigraphic control, summary
369 logs, and detail on hemipelagic mud deposits, is available online at
370 www.geosociety.org/pubs/ft2014.htm, or on request from editing@geosociety.org or
371 Documents Secretary, GSA, P.O. Box 9140, Boulder, CO 80301, USA.